

Electronic Structure and UV Absorption Spectra of 2-Pyridylacetylenes: An Intramolecular Orbital Interaction between the n Orbital on the Nitrogen Atom of the Pyridine Ring and the In-plane π Orbital of the Ethynylene Group

Jun Okubo,* Hiraku Shinozaki, Toshiyuki Koitabashi, and Ryo Yomura

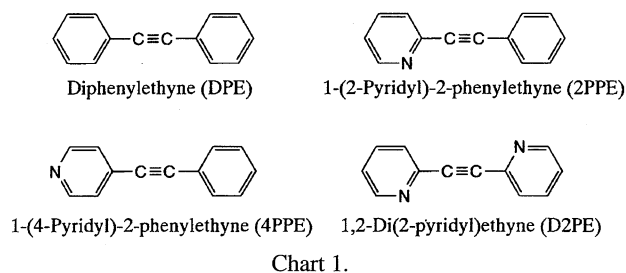
Department of Natural Science for General Education, Faculty of Engineering, Tokyo Denki University,
Muzai Gakuendai, Inzai, Chiba 270-13

(Received August 11, 1997)

The UV absorption spectra of some pyridylacetylenes were measured in various media at room temperature and 77 K, and the origin of the electronic absorption bands of these compounds was clarified compared with the results of MO calculations. For instance, it has been found that the 304.6, 271.7, 221, and 216 nm bands of 1-(2-pyridyl)-2-phenylethyne in cyclohexane can be assigned to the calculated $S_1 \leftarrow S_0$, $S_5 \leftarrow S_0$, $S_9 \leftarrow S_0$, and $S_{10} \leftarrow S_0$ transitions, respectively, in which the observed 271.7 nm band ($S_5 \leftarrow S_0$) is ascribed as a new type transition from the n orbital on the aza-nitrogen atom of the pyridine ring to the in-plane π^* orbital on the sp-carbon atoms of the ethynylene group. Furthermore, it is revealed that the observed 259.6 nm band of 1,2-di(2-pyridyl)ethyne (D2PE) can also be assigned to a new type of transition caused by weak interactions between the n orbitals and the in-plane π orbital of the ethynylene group. This result indicates that two n orbitals of the terminal pyridine rings of D2PE may interact with each other via the central in-plane π orbital.

The inter- and intramolecular interactions between the σ -electronic system or nonbonding orbital and the π electronic system have been of interest in the studies of the reaction mechanism of alkynes or alkenes with electrophilic or nucleophilic reagents.^{1–3)} It is well-known that these molecular interactions including the hydrogen bond play an important role in molecular recognition. Recently, Pilkington et al. find the attractive intramolecular interactions between the alkyne sp-hybridized carbon atoms and the carbonyl oxygen atoms of 2,2'-ethynylendibenzoic acid by a precise analysis of the single-crystal X-ray diffraction.⁴⁾ They also reported that a unique interaction between an alkynyl group and nitro oxygen atom in 1-(2-aminophenyl)-2-(2-nitrophenyl)ethyne leads to a *trans*-bend in the alkyne.⁵⁾ In our previous paper,⁶⁾ we discussed the origin of the He I photoelectron bands of some pyridylacetylenes based on the results of MO calculations; also, through the process of the band assignment, we have suggested that 2-ethynylpyridine shows a very weak interaction between the nonbonding electron pair on the nitrogen atom of the pyridine ring and the in-plane π -orbital of the ethynylene group. This weak interaction brings about a slight shift in the ionization energy of the molecular orbital.

In this investigation, 1-(2-pyridyl)-2-phenylethyne (abbreviated to 2PPE), 1-(4-pyridyl)-2-phenylethyne (4PPE) and 1,2-di(2-pyridyl)ethyne (D2PE) were prepared (Chart 1), and the UV absorption spectra were measured in various media at room temperature and 77 K. In conjunction with a modified PPP calculation,^{7–10)} the origin of each electronic absorption band of the pyridylacetylenes has been clarified; we discuss the possibility of an intramolecular orbital inter-



action between the in-plane π orbital of the sp-hybridized carbon atom and the n orbital on the nitrogen atom of the pyridine ring.

Experimental

Measurements. The UV absorption spectra were measured with a Hitachi UV-3210 spectrophotometer, and the spectra in rigid matrix at 77 K were recorded on the above-mentioned spectrophotometer equipped with a quartz dewar vessel EDN-3 (Eikohsya Co., Ltd.). IR and NMR spectra were measured with a JEOL JIR-RFX3001 and a JEOL FX90Q spectrophotometers, respectively.

Materials. Diarylethyne were prepared by employing the typical procedure with a palladium(II)–Cu(I) catalytic system.¹¹⁾

1-(2-Pyridyl)-2-phenylethyne (2PPE).¹²⁾ A mixture of 2-bromopyridine (4.76 g, 30 mmol), phenylacetylene (3.73 g, 37 mmol), dichlorobis(triphenylphosphine) palladium(II) (0.14 g, 0.2 mmol) and copper(I) iodide (0.06 g, 0.3 mmol) in 20 mL of diethylamine was stirred for 1 h under N_2 . After diethylamine was removed in vacuo, a saturated NH_4Cl solution (15 mL) was added. The mixture was extracted twice with diethyl ether (20 mL). The combined organic layers were washed with a saturated NH_4Cl solution, dried over $MgSO_4$, and evaporated under reduced pressure. The residue

was purified by column chromatography on silica gel (ether:hexane = 3:7). This was followed by recrystallization from a 1:1 mixture of ethanol and hexane in a refrigerator to give 2PPE (3.33 g, 62%) as a colorless solid. mp 30.5–31.5 °C; $^1\text{H NMR}$ (90 MHz, CDCl_3) δ_{H} = 7.04–7.38 (m, 4H), 7.40–7.65 (m, 4H), 8.53 (d, J = 5.4 Hz, 1H); $^{13}\text{C NMR}$ (23 MHz, CDCl_3) δ_{C} = 149.73, 143.13, 135.87, 131.72, 128.96, 128.12 (strong), 126.87, 122.49 (strong), 121.97, 88.95, 88.44; IR (KBr) 2218 cm^{-1} ($\text{C}\equiv\text{C}$).

1-(4-Pyridyl)-2-phenylethyne (4PPE). 4PPE (1.71 g, 96%) was obtained from phenylacetylene (1.02 g, 10 mmol) and 4-bromopyridine hydrochloride (2.33 g, 12 mmol). The reaction was carried out at r.t. for 3 h followed by refluxing for 2 h. Mp 92–93 °C; $^1\text{H NMR}$ (90 MHz, CDCl_3) δ_{H} = 8.56 (broad, 2H), 7.58–7.30 (m, 7H); $^{13}\text{C NMR}$ (23 MHz, CDCl_3) δ_{C} = 149.70, 131.79, 131.36, 129.14, 128.44, 125.45, 122.02, 93.89, 86.61; IR (KBr) 2222 cm^{-1} ($\text{C}\equiv\text{C}$).

1,2-Di(2-pyridyl)ethyne (D2PE). D2PE (0.30 g, 16%) was obtained from the reaction of 2-pyridylethyne⁶⁾ (1.11 g, 11 mmol) and 2-bromopyridine (1.90 g, 12 mmol) at reflux for 4 h. Mp 70–71 °C; $^1\text{H NMR}$ (90 MHz, CDCl_3) δ_{H} = 8.64 (dt, J = 5.0, 1.4 Hz, 2H), 7.80–7.40 (m, 4H), 7.30–7.20 (m, 2H); $^{13}\text{C NMR}$ (23 MHz, CDCl_3) δ_{C} = 150.06, 142.61, 136.11, 127.66, 123.75, 87.78; IR (KBr) 2162 cm^{-1} ($\text{C}\equiv\text{C}$).

MO Calculation. Molecular-orbital calculations for the π -electron system were carried out by a modified PPP method,^{7–10)} which can treat two π - and n -orbitals that are perpendicular to each other at the same time. In these calculations, the valence-state ionization energy ($I_{\text{p}}(r)$) and electron affinity ($E_{\text{a}}(r)$) of atom r were used as follows: $I_{\text{p}}(\text{C})$ = 11.22, $E_{\text{a}}(\text{C})$ = 0.62, $I_{\text{p}}(\text{N})$ = 14.16, $E_{\text{a}}(\text{N})$ = 1.34, $I_{\text{p}}(\text{N}^{\cdot-})$ = 25.00 and $E_{\text{a}}(\text{N}^{\cdot-})$ = 10.00 eV. The resonance integral (β_{rs}) between atoms r and s was computed by means of the variable β approximation of Nishimoto–Forster,¹³⁾ and all differential overlap integrals were conventionally neglected. All singly excited configurations were taken into account in the CI calculation. The geometrical parameters of the pyridylacetylenes were taken from X-ray diffraction data.^{14,15)}

Results and Discussion

The UV absorption spectra of diphenylethyne (DPE) is shown in Fig. 1; the dotted line is the measured value in ethanol, and the solid line in cyclohexane. DPE shows absorption bands at 298.3, 289.3, 280.9, 273.4, and 265.9 nm in cyclohexane, in which the 289.3, 280.9, 273.4, and 265.9 nm bands

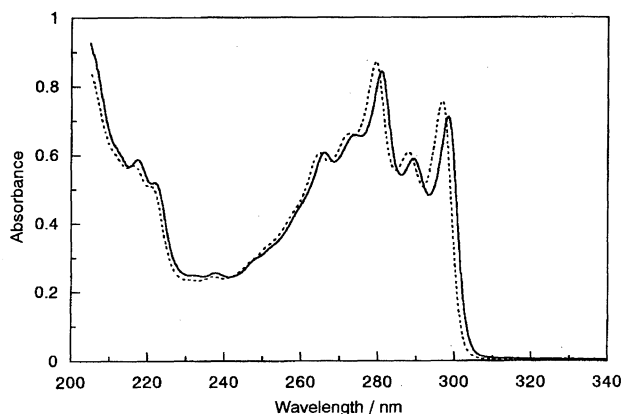


Fig. 1. The UV absorption spectra of diphenylethyne (DPE) in ethanol (---) and cyclohexane (—).

are considered to be the vibronic bands of the 0–0 band at 298.3 nm. Furthermore, weak bands are observed at 222 and 217.4 nm. To know the origin of these UV absorption bands of DPE, we performed a modified PPP calculation; the results of which are presented in Table 1 compared with the experimental data. In this calculation, the ordinary out-of-plane π orbitals and the in-plane π orbitals of the ethynylene groups were taken into account at the same time. Judging from the transition energies and intensities, the observed 298.3, 222, and 217.4 nm bands are reasonably assigned to the calculated $S_1 \leftarrow S_0$ ($^1\text{B}_{1u} \leftarrow ^1\text{A}_g$), $S_7 \leftarrow S_0$ ($^1\text{B}_{2u} \leftarrow ^1\text{A}_g$), and $S_8 \leftarrow S_0$ ($^1\text{B}_{1u} \leftarrow ^1\text{A}_g$) transitions, respectively, and the calculated results are in fairly agreement with the observed ones. The 298.3, 222, and 217.4 nm bands correspond to the transitions, $^1\text{B}_{2u} \leftarrow ^1\text{A}_g$, $^1\text{B}_{1u} \leftarrow ^1\text{A}_g$, and $^1\text{B}_{2u} \leftarrow ^1\text{A}_g$ (the Y -axis is selected along the long molecular axis), respectively, which are previously assigned by Tanizaki et al.¹⁶⁾

The absorption spectra of 4PPE and 2PPE are shown in Figs. 2a and 2b, respectively, which were measured under the same condition as in the case of DPE. Since the π systems of these compounds are isoelectronic with that of DPE, the electronic transition energies and intensities of 4PPE and 2PPE are considered to succeed essentially to those of DPE. The 0–0 band of the first electronic transition of 4PPE appears

Table 1. The Calculated and Observed Transition Energies, Intensities, and Polarizations for Diphenylethyne (DPE)

	Transition energy/nm		Intensity		Polarization direction	
	Calcd	Obsd ^{a)}	Calcd	Obsd ^{b)}	Calcd ^{c)}	Obsd ^{d)}
$S_1(^1\text{B}_{1u})$	321.5	298.3	1.2041	2.47	0.00	L
$S_2(^1\text{B}_{2u})$	297.1		forb.			
$S_3(^1\text{B}_{3g})$	296.8		forb.			
$S_4(^1\text{A}_u)$	235.1		forb.			
$S_5(^1\text{A}_u)$	233.4		forb.			
$S_6(^1\text{B}_{3g})$	225.5		forb.			
$S_7(^1\text{B}_{2u})$	223.0	222	0.6661	1.85	90.00	S
$S_8(^1\text{B}_{1u})$	214.0	217.4	0.2928	2.05	0.00	L
$S_9(^1\text{B}_{1u})$	201.3		forb.			
$S_{10}(^1\text{B}_{2u})$	199.5		forb.			

a) Measured in cyclohexane. b) Molar absorptivity/ $10^4 \text{ dm}^3 \text{ mol}^{-1} \text{ cm}^{-1}$. c) The angle in degree with respect to the long molecular axis. d) Taken from Ref. 16. L; Long molecular axis, S; Short molecular axis. forb.; Forbidden transition.

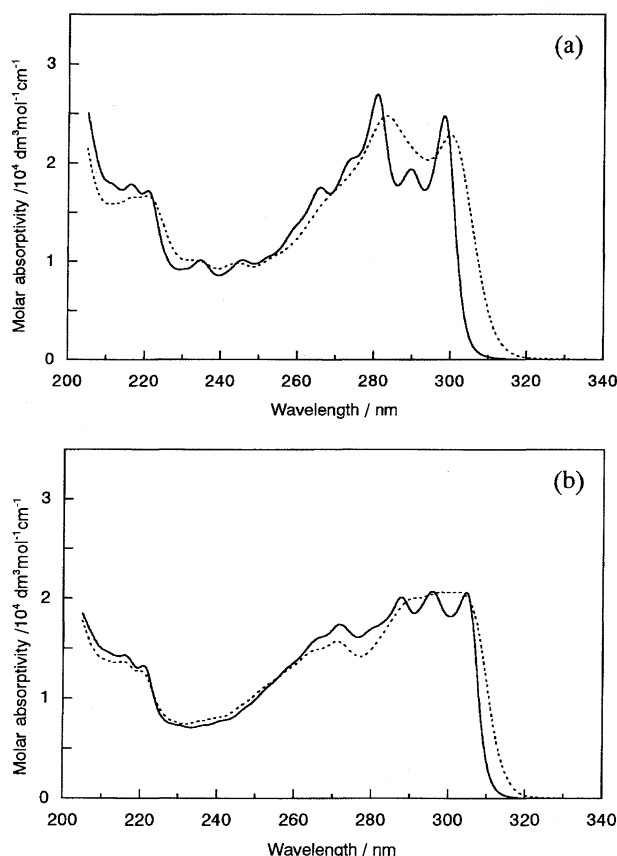


Fig. 2. The UV absorption spectra of 1-(4-pyridyl)-2-phenylethyne (4PPE) (a) and 1-(2-pyridyl)-2-phenylethyne (2PPE) (b) in ethanol (---) and cyclohexane (—).

at 298.8 nm in cyclohexane, and the vibronic bands at 289.6, 281.0, 273.5, and 265.7 nm, involving the $\text{C}\equiv\text{C}$ stretching mode (2060 cm^{-1}). The absorption bands in the higher energy side are observed at 221 and 216.5 nm, which are considered to correspond to the 222 and 217.4 nm bands of DPE, respectively. Furthermore, two weak bands appear at 245.6 and 235.0 nm. These two bands may be attributed to an isolated transition from the 298.8 and 221 nm bands. Upon going from in cyclohexane to in ethanol, the first band system of 4PPE becomes broader, and slightly red-shifted, except for the 245.6 nm band. The external shape of the absorption spectrum of 4PPE is, at a glance, very similar to that of DPE, and it seems that the electronic nature of 4PPE succeeds essentially to that of DPE.

On the other hand, 2PPE shows the first absorption band at 304.6 nm in cyclohexane, which accompanies the vibronic bands at 295.7 and 287.7 nm on the higher energy side. The absorption bands derived from the 222 and 217.4 nm bands of DPE are observed at 221 and 216 nm, respectively. In addition, a new band appears at 271.7 nm. Although a weak band corresponding to the 245.6 nm one of 4PPE is not apparent in the wavelength region 230–250 nm, 2PPE exhibits a very small band in the wavelength region. The first absorption band system of 2PPE is sharpened upon going from in ethanol to in cyclohexane, and the second band at 271.7 nm is somewhat sharpened and remains almost at the

same position. The above results indicate that 2PPE shows at least two electronic transitions in the wavelength region 260–320 nm, and 4PPE shows a single a transition in the wavelength region.

In order to obtain additional information on the nature of the 271.7 nm band of 2PPE, the UV absorption spectra were measured in EPA (diethyl ether : isopentane : ethanol = 5 : 5 : 2) at room temperature (solid line) and 77 K (dotted line) (Fig. 3). The absorption spectrum at room temperature consists of bands at 302.4, 294.8, 286.1, 271.0, and 264.3 nm. The spectrum is considerably sharpened with lowering the temperature, and the shoulder bands at room temperature change to distinct fine structures at 77 K. The peaks shift to the lower energy side, i.e., the 302.4, 294.8, and 286.1 nm bands at room temperature appear at 310.6, 301.3, and 292.5 nm at 77 K. The bands around 220, 215, and 210 nm at room temperature are also red-shifted by ca. 3.5 nm at 77 K, and the 271.0 and 264 nm bands at room temperature are slightly red-shifted only by ca. 1 nm with lowering temperature. This temperature dependence of the absorption bands may also indicate that 2PPE shows two electronic transitions in the 260–320 nm wavelength region, which are different from each other regarding their electronic nature.

MO calculations were performed for 4PPE and 2PPE in the same way as for DPE; the calculated and observed results are summarized in Table 2. From the transition energies and intensities, it is obvious that the 298.8, 221, and 216.5 nm bands of 4PPE can be assigned to the $\text{S}_1 \leftarrow \text{S}_0$ ($^1\text{A}_1 \leftarrow ^1\text{A}_1$), $\text{S}_8 \leftarrow \text{S}_0$ ($^1\text{B}_2 \leftarrow ^1\text{A}_1$), and $\text{S}_9 \rightarrow \text{S}_0$ ($^1\text{A}_1 \leftarrow ^1\text{A}_1$) transitions, respectively. In this calculated result, the oscillator strength of the $\text{S}_7 \leftarrow \text{S}_0$ ($^1\text{B}_2 \leftarrow ^1\text{A}_1$) transition of 4PPE is computed to be 0.1124, and presumably the low intense band at 245.6 nm may be attributed to this calculated transition. As for 2PPE, the first absorption band at 304.6 nm is reasonably assigned to the $\text{S}_1 \leftarrow \text{S}_0$ transition, and the 221 and 216 nm bands to the $\text{S}_9 \leftarrow \text{S}_0$ and $\text{S}_{10} \leftarrow \text{S}_0$ transitions, respectively. On the other hand, the transition corresponding to the additional band which appeared at 271.7 nm is not found in this calculation.

In present stage, although the origin of the second tran-

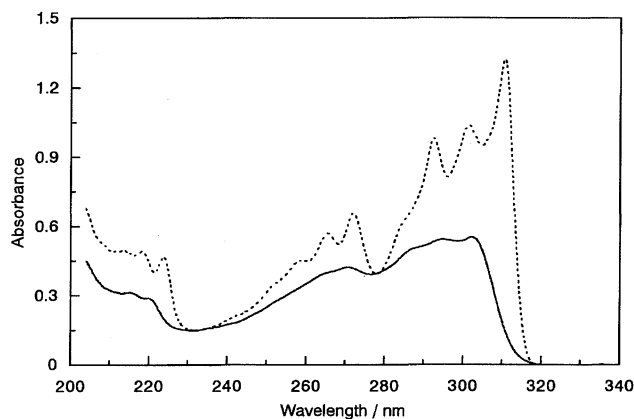


Fig. 3. The UV absorption spectra of 2PPE in EPA at room temperature (—) and 77 K (---).

Table 2. The Calculated and Observed Transition Energies, Intensities, and Polarizations for 4PPE and 2PPE

4PPE (C_{2v} Symmetry)					
	Transition energy/nm		Intensity		P.D. ^{c)}
	Calcd	Obsd ^{a)}	Calcd	Obsd ^{b)}	Calcd
S ₁ (¹ A ₁)	317.4	298.8	1.1762	2.50	0.00
S ₂ (¹ B ₂)	296.9		0.0003		90.00
S ₃ (¹ B ₁)	293.7		forb.		
S ₄ (¹ B ₂)	291.9		0.0218		90.00
S ₅ (¹ A ₁)	232.3		0.0022		0.00
S ₆ (¹ A ₁)	228.6		0.0051		0.00
S ₇ (¹ B ₂)	224.4	245.6	0.1124	1.00	90.00
S ₈ (¹ B ₂)	221.3	221	0.4947	1.75	90.00
S ₉ (¹ A ₁)	213.5	216.5	0.3446	1.80	0.00
S ₁₀ (¹ A ₂)	212.8		forb.		
S ₁₁ (¹ B ₂)	202.1		forb.		
S ₁₂ (¹ B ₂)	198.3		0.0600		90.00

2PPE (C_s Symmetry)					
	Transition energy/nm		Intensity		P.D. ^{c)}
	Calcd	Obsd ^{a)}	Calcd	Obsd ^{b)}	Calcd
S ₁	322.4	304.6	1.1121	2.20	-0.58
S ₂	296.8		0.0002		51.92
S ₃	296.3		forb.		
S ₄	284.5		0.0805		
S ₅	250.2	? 271.7	forb.	? 1.88	-21.10
S ₆	235.5		0.0175		-85.29
S ₇	231.2		0.0074		-53.68
S ₈	228.1		forb.		
S ₉	223.9	221	0.2738	1.41	-87.09
S ₁₀	216.3	216	0.3129	1.55	62.75
S ₁₁	210.8		0.1700		-25.04
S ₁₂	199.8		0.0003		-33.73

a) Measured in cyclohexane. b) Molar absorptivity/ $10^4 \text{ dm}^3 \text{ mol}^{-1} \text{ cm}^{-1}$. c) The angle of polarization direction in degree with respect to the long molecular axis. forb.; Forbidden transition.

sition of 2PPE is not clear, the following two possibilities may be assumed. Firstly, the 271.7 nm band in cyclohexane is assigned to the calculated $S_4 \leftarrow S_0$ or $S_6 \leftarrow S_0$ transition with a low oscillator strength, which becomes electronically allowed along with a decrease in the molecular symmetry by replacing the *ortho*-position of the phenyl ring by a heterocyclic nitrogen atom. Secondly, in consequence of an intramolecular orbital interaction between the nonbonding orbital on the aza-nitrogen atom and the in-plane π orbital in the ethynylene group, the transition becomes stronger in intensity, and the 271.7 nm band originates from this intensified electronic transition. As for the former possibility, it is considered that the oscillator strength of the $S_4 \leftarrow S_0$ or $S_6 \leftarrow S_0$ transition is too weak to be assigned to the observed 271.7 nm band, because the ratio of the area intensities of the first and second band systems in wavenumber as abscissa is about 5:2 in EPA at 77 K (Fig. 3). In order to inspect the latter possibility, we performed MO calculations for 2PPE, in which the interaction between the nonbonding orbital of the pyridine ring and the in-plane π orbital in the ethynylene group were taken into account. A weak through-space interaction is assumed in this calculation, and the transition energies and

the oscillator strengths of 2PPE are computed again by the use of various resonance integrals ($\beta_{n-\text{Csp}} = 0.0 \text{--} 0.8 \text{ eV}$). The calculated results are presented in Fig. 4. The height of the bar is proportional to the oscillator strength of the transition, and the circle denotes a forbidden transition. As can be seen from this figure, the first electronic transition is slightly shifted to the lower energy side along with an increase in the absolute value of $\beta_{n-\text{Csp}}$, and the intensity is scarcely changed, whereas the $S_5 \leftarrow S_0$ transition is intensified and shifted to the higher energy side with an increase in the absolute value of $\beta_{n-\text{Csp}}$. The oscillator strength of the $S_5 \leftarrow S_0$ transition is computed to be 0.2062, $\beta_{n-\text{Csp}}$, being assumed to be -0.6 eV ; it thus seems natural to assign the 271.7 nm band of 2PPE to the $S_5 \leftarrow S_0$ transition. Although the magnitude of this $\beta_{n-\text{Csp}}$ value is tentatively estimated, the value is in accordance with that evaluated by analyses of the photoelectron spectrum of 2-pyridylethyne.⁶⁾

The MO calculated results by use of the resonance integral ($\beta_{n-\text{Csp}} = -0.6 \text{ eV}$) between the n orbital of pyridine ring and the in-plane π orbital in the ethynylene group are summarized in Table 3 compared with the observed ones. The 304.6, 221, and 216 nm bands of 2PPE are assigned to the

$S_1 \leftarrow S_0$, $S_9 \leftarrow S_0$, and $S_{10} \leftarrow S_0$ transitions, respectively, and the 271.7 nm band to the $S_5 \leftarrow S_0$ transition. Here, the calculated forbidden $S_3 \leftarrow S_0$ and $S_8 \leftarrow S_0$ transitions are ordinary

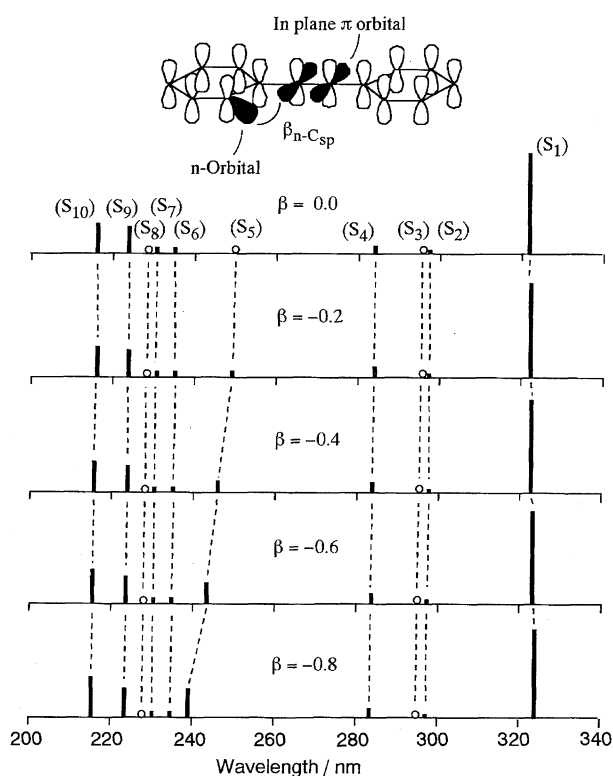


Fig. 4. Energy correlation diagram of the calculated transitions for the various resonance integrals β_{n-Csp} between the n orbital on the nitrogen atom of the pyridine ring and the in-plane π orbital in the ethynylene group.

Table 3. The Calculated and Observed Transition Energies, Intensities, and Polarizations for 2PPE

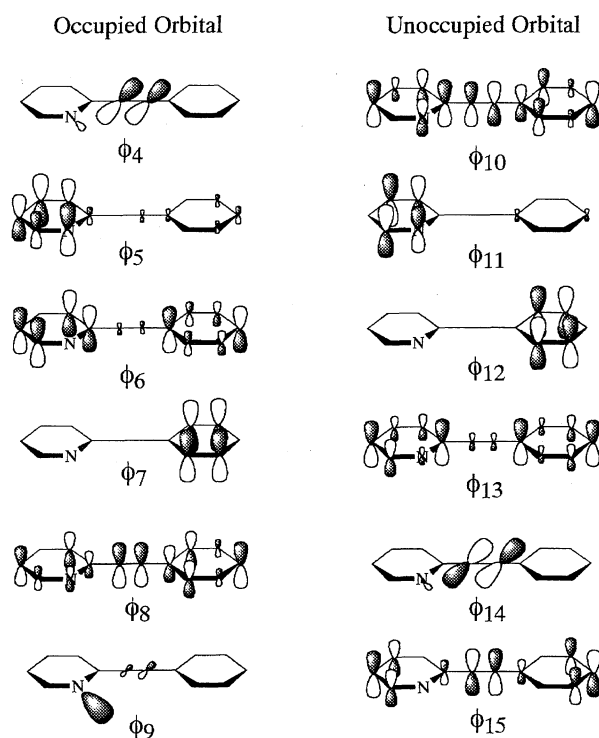
A weak through-space interaction between the n orbital on the nitrogen atom of pyridine ring and the in-plane π orbital of the ethynylene group is taken into account in this calculation, and the value of the resonance integral β_{n-Csp} is assumed to be -0.6 eV.

	Transition energy/nm		Intensity		P.D. ^{c)}
	Calcd	Obsd ^{a)}	Calcd	Obsd ^{b)}	Calcd
S_1	323.3	304.6	1.0601	2.20	-0.66
S_2	296.7		0.0002		55.53
S_3	293.2		forb.		
S_4	284.4		0.0752		-22.90
S_5	243.1	271.7	0.2062	1.88	-2.81
S_6	235.5		0.0182		-80.87
S_7	230.9		0.0248		-32.81
S_8	227.5		forb.		
S_9	223.9	221	0.2875	1.41	-85.35
S_{10}	215.5	216	0.3679	1.55	49.90
S_{11}	210.8		0.1568		-27.00
S_{12}	199.8		0.0003		-45.69

a) Measured in cyclohexane. b) Molar absorptivity/ $10^4 \text{ dm}^3 \text{ mol}^{-1} \text{ cm}^{-1}$. c) The angle of polarization direction in degree with respect to the long molecular axis. forb.; Forbidden transition.

$n-\pi^*$ ones.

The total wavefunctions (Ψ_1 , Ψ_5 , Ψ_9 , and Ψ_{10}) in the singlet excited states, corresponding to the observed 304.6, 271.7, 221, and 216 nm bands of 2PPE, and the diagrammatic representation of the MOs contributed to the lower configuration interaction (CI) are presented in Fig. 5. The height of the orbital is roughly proportional to the magnitude of the AO coefficient. The wavefunction Ψ_1 is contributed mainly to the χ_{8-10} configuration, whose CI coefficient is 0.952, thus indicating that the Ψ_1 can be ascribed as the transition from MO ϕ_8 to ϕ_{10} . It is thus found that the first absorption band corresponding to Ψ_1 can be regarded as an ordinary $\pi-\pi^*$ transition delocalized over the whole molecule. On the other hand, Ψ_5 (the 271.7 nm band) is mainly contributed to the configuration χ_{9-14} , whose CI coefficient is 0.950. The AO coefficient in the MO ϕ_9 is localized almost on the nonbonding orbital on the aza-nitrogen atom of the pyridine ring, whereas those in the MO ϕ_{14} are localized on the in-plane π^* orbital in the ethynylene group. That is, it is found that the observed 271.7 nm band of 2PPE may be regarded as a transition from the n orbital of the pyridine ring to the in-



$$\Psi_1 = 0.952 \chi_{8-10} + 0.135 \chi_{8-11} - 0.117 \chi_{6-11} + \dots$$

$$\Psi_5 = 0.950 \chi_{9-14} + 0.160 \chi_{5-10} - 0.124 \chi_{8-13} + \dots$$

$$\Psi_9 = 0.705 \chi_{7-10} + 0.674 \chi_{8-12} - 0.211 \chi_{5-11} + \dots$$

$$\Psi_{10} = -0.559 \chi_{8-11} + 0.551 \chi_{5-10} - 0.346 \chi_{7-12} + \dots$$

Fig. 5. Total wavefunctions, Ψ_1 , Ψ_5 , Ψ_9 , and Ψ_{10} in the excited states of 2PPE, and the diagrammatic representation of MOs concerning the main contributors of the electronic transitions.

plane π^* orbital, which is intensified through the interaction between the n orbital and the in-plane π orbital in the ethynylene group. It may also be interpreted that the $S_5 \leftarrow S_0$ transition is intensified by a mixing of the χ_{9-14} configuration and the lower ones as the result of a shift of the anti-bonding orbital ϕ_9 consisting of the n and in-plane π orbitals to the higher energy side.

In analogy with the above consideration, the 221 nm band (Ψ_6) is derived from the intramolecular charge-transfer transition between the ethynylpyridine moiety and the phenyl ring, and the 216 nm band (Ψ_{10}) derived from the transition between the pyridine ring and the phenylethyne moiety.

For a further examination of the above discussion, the UV absorption spectrum of 1,2-di(2-pyridyl)ethyne (D2PE) was measured in EPA at room temperature and 77 K, as shown in Fig. 6. In the spectrum measured at room temperature, the absorption bands appear at 305.9, 297.2, and 289.3 nm.

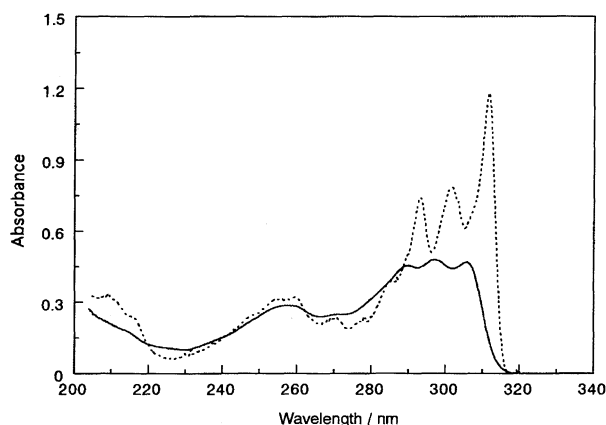


Fig. 6. The UV absorption spectra of di(2-pyridyl)ethyne (D2PE) in EPA at room temperature (—) and 77 K (---).

Table 4. The Calculated and Observed Transition Energies, Intensities, and Polarizations for D2PE ($\beta_{n-Csp} = -0.6$ eV)

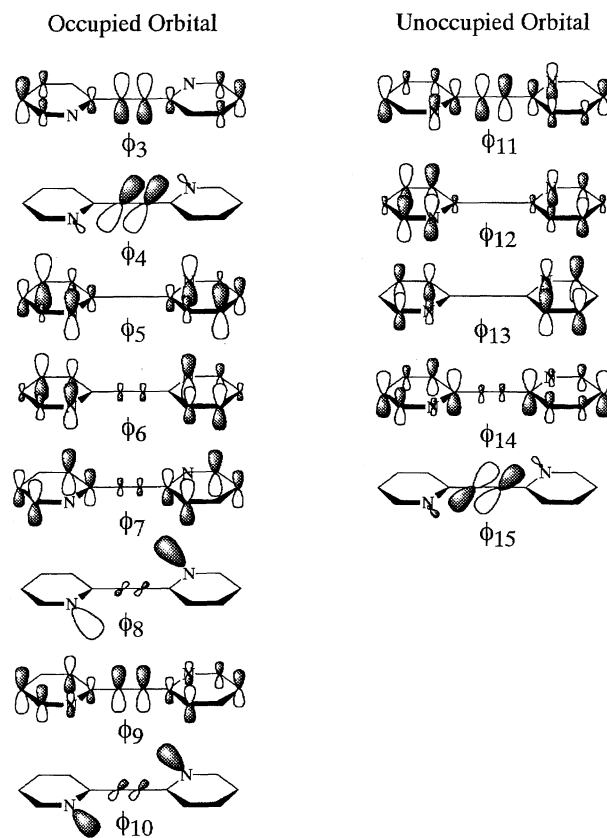
	Transition energy/nm		Intensity		P.D. ^{c)}
	Calcd	Obsd ^{a)}	Calcd	Obsd ^{b)}	Calcd
$S_1(^1B_u)$	324.3	311.8	0.9530	1.20	-1.71
$S_2(^1B_g)$	301.4		forb.		
$S_3(^1A_u)$	294.1		forb.		
$S_4(^1A_g)$	287.9		0.0000		-17.10
$S_5(^1B_u)$	279.7	277.6	0.1090	0.20	-30.44
$S_6(^1B_u)$	245.2	259.6	0.4255	0.29	-7.21
$S_7(^1A_g)$	235.8		0.0000		6.08
$S_8(^1A_g)$	235.6		0.0000		29.3
$S_9(^1B_g)$	232.4		forb.		
$S_{10}(^1A_u)$	227.2		forb.		
$S_{11}(^1A_g)$	227.2		0.0000		25.01
$S_{12}(^1B_u)$	215.3	216	0.6093	0.24	58.34
$S_{13}(^1A_g)$	213.0		0.0016		49.86
$S_{14}(^1B_u)$	208.1	209.2	0.1386	0.31	-45.24

a) Measured in EPA at 77 K. b) Absorbance in EPA at 77 K.

c) The angle of polarization direction in degree with respect to the long molecular axis. forb.; Forbidden transition.

The broad band is observed around 257 nm, and a shoulder one around 214 nm. The intensity of the first absorption band system is considerably intensified with lowering the temperature, and the 0-0 band is observed at 311.8 nm at 77 K, accompanying vibronic bands at 301.7 and 293.2 nm. The bands around 214 nm at room temperature are observed as shoulders at 216 and 209.2 nm at 77 K, corresponding to those in the higher wavelength region for DPE, 4PPE, and 2PPE. The broad band around 257 nm splits to two peaks at 259.6 and 255 nm at 77 K. The observed 259.6 nm band may be derived from the 271.7 nm band of 2PPE. In addition, two weak bands appear at 277.6 and 270.0 nm at 77 K, which are not found in the cases of DPE, 2PPE, and 4PPE.

Using the resonance integral ($\beta_{n-Csp} = -0.6$) between the n and in-plane π orbitals, MO calculation for D2PE was performed, and the results were presented in Table 4. The calculated results are in good agreement with the observed ones



$$\Psi_1 = -0.932 \chi_{9-11} + 0.163 \chi_{9-13} - 0.155 \chi_{7-12} + \dots$$

$$\Psi_6 = 0.956 \chi_{10-15} - 0.165 \chi_{9-13} + 0.160 \chi_{9-11} + \dots$$

$$\Psi_{12} = 0.625 \chi_{9-13} - 0.589 \chi_{6-11} - 0.200 \chi_{5-13} + \dots$$

$$\Psi_{14} = 0.442 \chi_{6-13} - 0.429 \chi_{3-11} - 0.394 \chi_{5-12} + 0.366 \chi_{6-11} + 0.342 \chi_{7-14} + \dots$$

Fig. 7. Total wavefunctions, Ψ_1 , Ψ_6 , Ψ_{12} , and Ψ_{14} in the excited states of D2PE, and the diagrammatic representation of MOs concerning the main contributors of the electronic transitions.

judging from the transition energy and the oscillator strength. The observed 311.8, 259.6, 216, and 209.2 nm bands are assigned to the $S_1 \leftarrow S_0$ ($^1B_u \leftarrow ^1A_g$), $S_6 \leftarrow S_0$ ($^1B_u \leftarrow ^1A_g$), $S_{12} \leftarrow S_0$ ($^1B_u \leftarrow ^1A_g$), and $S_{14} \leftarrow S_0$ ($^1B_u \leftarrow ^1A_g$) transitions, respectively. The weak band observed at 277.6 nm may be assigned to the calculated $S_5 \leftarrow S_0$ ($^1B_u \leftarrow ^1A_g$) transition. Figure 7 shows the total wavefunctions (Ψ_1 , Ψ_6 , Ψ_{12} , and Ψ_{14}) in the excited states of D2PE and the diagrammatic representation of the MOs concerning the main contributors of the electronic transitions. Ψ_1 is contributed mainly to the χ_{9-11} configuration, whose CI coefficient is -0.932 , thus indicating that the first absorption band of D2PE can be regarded as a $\pi-\pi^*$ transition delocalized over the whole molecule. Ψ_6 , corresponding to the 259.6 nm band, is mainly contributed to the χ_{10-15} configuration, whose CI coefficient is 0.956 . The AO coefficient in the MO ϕ_{10} is localized almost on the nonbonding orbitals on the aza-nitrogen atoms of the terminal pyridine rings, whereas that in the MO ϕ_{15} is localized on the in-plane π^* orbital in the ethynylene group. That is, it is found that the 259.6 nm band of D2PE can be also regarded as a transition from the two n orbitals to the in-plane π^* orbital in the ethynylene group. The main contributors of Ψ_{12} corresponding to the 216 nm band are of configurations, χ_{9-13} (39%), χ_{6-11} (35%), and χ_{5-13} (4%), and this band is ascribed as a mixture of the localized transition in the terminal pyridine rings and the charge-transfer transitions between the pyridine rings and the central ethyne group. In the above discussions, it is particularly interesting that two n orbitals of D2PE may interact with each other via the central in-plane π orbital in the ethynylene group.

The authors are grateful to the Saneyoshi Scholarship Foundation and Tokyo Denki University, Research Institute for Technology for their financial supports.

References

- 1) S. R. Naidu and S. G. Peeran, *Tetrahedron*, **31**, 465 (1975).
- 2) J. S. Filippo, Jr., A. F. Sowinski, and L. J. Romano, *J. Org. Chem.*, **40**, 3463 (1975).
- 3) R. Köster, K. -H. Krämer, and R. Liedtke, *Liebigs Ann. Chem.*, **1973**, 1241.
- 4) M. Pilkington, S. Tayyip, and J. D. Wallis, *J. Chem. Soc., Perkin Trans. 2*, **1994**, 2481.
- 5) M. Pilkington, J. D. Wallis, J. D. Smith, and J. A. K. Howard, *J. Chem. Soc., Perkin Trans. 2*, **1996**, 1849.
- 6) J. Okubo, H. Shinozaki, M. Kubota, and T. Kobayashi, *J. Electron Spectrosc. Relat. Phenom.*, **77**, 276 (1996).
- 7) M. Kobayashi, T. Hoshi, J. Okubo, H. Hiratsuka, T. Harazono, and M. Nakagawa, *Bull. Chem. Soc. Jpn.*, **57**, 2905 (1984).
- 8) T. Hoshi, J. Okubo, I. Ono, S. Watanabe, H. Inoue, T. Sakurai, and M. Kobayashi, *Nippon Kagaku Kaishi*, **1990**, 655.
- 9) T. Hoshi, T. Kawashima, J. Okubo, and M. Yamamoto, *J. Chem. Soc., Perkin Trans. 2*, **1986**, 1147.
- 10) T. Hoshi, J. Okubo, M. Kobayashi, and Y. Tanizaki, *J. Am. Chem. Soc.*, **108**, 3867 (1986).
- 11) a) K. Sonogashira, Y. Tohda, and N. Hagihara, *Tetrahedron Lett.*, **50**, 4467 (1975); b) L. D. Ciana and A. Haim, *J. Heterocycl. Chem.*, **21**, 607 (1984); c) S. J. Havens and P. M. Hergenrother, *J. Org. Chem.*, **50**, 1763 (1985); d) L. Brandsma, "Preparative Acetylenic Chemistry," Elsevier, New York (1988), p. 177.
- 12) M. A. Dela Rossa, E. Velarde, and A. Guzman, *Synth. Commun.*, **20**, 2059 (1990).
- 13) K. Nishimoto and L. S. Forster, *Theor. Chim. Acta*, **3**, 407 (1965).
- 14) K. Swaminathan, U. C. Shinha, M. B. Kamath, S. S. Talbar, and R. Bohra, *Acta Crystallogr., Sect. C*, **C45**, 504 (1989).
- 15) J. R. Allen, M. J. Barrow, P. C. Beaumont, L. A. Macindoe, G. H. W. Milburn, and A. R. Werninck, *Inorg. Chim. Acta*, **148**, 85 (1988).
- 16) Y. Tanizaki, H. Inoue, T. Hoshi, and J. Shiraishi, *Z. Phys. Chem. N. F.*, **74**, 45 (1971).